Discussion

We have previously demonstrated the feasibility of the MSC-derived TEC approach for cartilage repair and showed the equivalent overall morphology and macro-scale compressive properties of TEC-mediated repair cartilage compared to normal cartilage (Ando *et al.*, 2007; Katakai *et al.*, 2009). However, we also pointed out the morphological abnormality in the superficial area of the TEC-mediated repair cartilage, with the predominance of fibro-cartilaginous tissue. The introduction of micro-scale biomechanical analysis along with detailed ultrastructural observations has enabled a more precise evaluation of zone-specific structure and function between normal and TEC-mediated repair cartilage. The present study specifically focused on the superficial zone of the repair cartilage and elucidated a number of unique characteristics of the tissue, morphologically and biomechanically. Grad *et al.* recently investigated the surface micro-scaled biomechanical properties of *in vitro* engineered cartilaginous tissues (Grad *et al.*, 2012). However, to our knowledge, the present study is the first demonstration of these unique functional abnormalities in the superficial zone of repair cartilage following implantation in a large animal model.

Morphologically, the combination of SEM with picrosirius red staining under polarised microscopy clearly demonstrated the difference in the surface structure of uninjured cartilage and the TEC-mediated repair tissue. SEM detected the dense paralleled fibrous bundle with the thickness of approximately 20 μm at the most superficial layer of uninjured articular cartilage. Interestingly, picrosirius red staining of the corresponding area showed the presence of a bright orange band, with approximately 100-150 μm thickness, aligned parallel with the surface of uninjured articular cartilage. Previous studies suggested that the thickness of the superficial tangential zone of articular cartilage has 10-20 % of the thickness of the whole cartilage (Mow *et al.* 1990) and the average thickness of porcine femoral articular cartilage is reported to be about 1 mm at 11 months of age, which corresponds to the period at the tissue sampling in the present study (10-11 months old) (Rieppo *et al.*. 2009). Thus, the thickness of the superficial tangential zone could be expected to be approximately 100-200 μm. The similarity in the thickness suggests that the surface orange band detected by picrosirius red staining may correspond to the superficial tangential zone and that the dense tangential fibrous band detected by SEM, which has less than 20 % of the thickness of the orange band, might be the superficial specialised structure involved in the superficial tangential zone. Notably, a bright red thin band with the thickness of 3 μm was observed at the very surface of uninjured cartilage. MacConaill first reported a thin bright line at the articular surface which consisted of parallel aligned fibres and termed it the lamina splendens (MacConaill, 1951). The width of the lamina splendens was reported to be 3.2-5.2 μm (Dunham, *et al.*, 1988) and 4-8 μm (Teshima *et al.*, 1995) in canine tibial plateau and human femoral head, respectively. Based on the similarity in the thickness, the red bright band presumably corresponds to the lamina splendens. On the other hand, SEM showed a thin fibre with the thickness of 3 μm at the surface of the TEC-treated cartilaginous tissues. However, picrosirius red staining did not show such a bright red or orange band at the tissue surface. Therefore, it is likely that the lamina splendens, or the structure of the superficial tangential zone, was not restored in the TEC-treated cartilaginous repair tissue. Significantly, inferior O'Driscoll scores in the TEC-mediated repair cartilaginous tissue at the superficial zone level may also be a reflection of the loss of the superficial structures. Thus, the lack of the lamina splendens coupled with the altered superficial tangential structure at the surface of the TEC-mediated repair cartilaginous tissue could be the most significant morphological finding in the present study.

The lamina splendens, together with the superficial tangential zone, is regarded as playing various important roles in maintaining the mechanical response of articular cartilage to load (Thambyah *et al.*, 2007, Hollander *et al.*, 2010), joint physiology – such as withstanding extrinsic compression and intrinsic swelling pressure – and facilitating joint lubrication (Teshima *et al.*, 1995). Therefore, the lack of these superficial structures could lead to a functional insufficiency at the superficial zone of the repaired cartilage in many properties, such as surface roughness, stiffness, lubrication and water retaining potential to control intrinsic swelling pressure. This may compromise the long term functionality of the repair tissue unless it continues to improve with time post-implantation.

In order to assess the potential functional insufficiency of the superficial zone of repair-cartilage, the atomic force microscopy (AFM) approach was employed. AFM has been reported to allow evaluation of the structure-mechanical property relationships at the surface of articular cartilage at the μm and nm scales (Stolz *et al.*, 2004; Hsieh *et al.*, 2008) and thus, to examine surface roughness and stiffness of the repair cartilage. There were no significant differences in the surface roughness between the TEC-mediated repair-cartilage and uninjured cartilage, while significantly lower micro-scale stiffness was detected in the TEC-mediated repair cartilage than in the uninjured cartilage. This result was in contrast with those of previous macro-scale compression assessments, where no significant differences between TEC-mediated repair cartilage and the uninjured cartilage were detected. Such findings indicate the lack of sensitivity of the macro approach and the importance of micro-scaled mechanical testing.

The proteoglycan 4 (PRG4) (lubricin) is a mucinous glycoprotein expressed in cartilage and one which is believed to play an important role in the boundary lubrication of articular cartilage (Swann *et al.*, 1977; Jay *et al.*, 1992). Therefore, expression and localisation of this molecule may estimate the lubrication properties of the TEC-mediated repair cartilage. In the present study, we demonstrated that PRG4 was similarly localised to the superficial zone of the TEC-mediated repair cartilage and in normal uninjured cartilage. In accordance with the similar localisation pattern of PRG4, there were no significant differences in the coefficient of friction between the TEC-mediated repair cartilage and the uninjured cartilage. We previously reported that the coefficient of friction of

the TEC-mediated repair cartilage was not significantly different from that of normal cartilage (Ando *et al.*, 2007). However, the results were obtained immediately after loading of the specimens, when the lubrication mode was thought to be a combination of hydrodynamic lubrication and boundary lubrication. Therefore, in the previous study, there might have been no clear effect of loading duration on the friction in which the boundary lubrication becomes dominant (Pickard *et al.*, 1998). In the present study, in order to eliminate that potential problem, we started the examination after 60 s of loading, and again obtained similar results. Taken together, the structural abnormality in the superficial zone of repair cartilage did not likely affect the surface localisation of PRG4 or the boundary lubrication properties of the repair cartilage.

Finally, we investigated the permeability (inverse relation to water retention capacity) of the repair cartilage. This capacity is considered essential to influence the crucial function of articular cartilage to control intrinsic swelling pressure (Mansour *et al.*, 1976). Interestingly, the TEC-mediated repair cartilage exhibited permeability similar to the uninjured cartilage at the level of the middle and deep zones, while higher permeability was detected in the repair cartilage at the surface/superficial zone. The permeability of normal cartilage has been reported to increase as one assesses deeper zones (Muir *et al.*, 1970), while the tendency of the TEC-mediated cartilaginous repair tissue was shown to be the opposite in the present studies. The present results clearly indicated that the superficial zone of the TEC-mediated repair cartilage exhibited significantly lower water retaining capacity. This is the first clear demonstration of a novel functional insufficiency involved in the superficial zone of the TEC-mediated repair cartilage, an insufficiency which could be closely related to the superficial structural abnormalities also detected in the present studies. A future detailed analysis in the structure and composition of the superficial tangential zone will be required to identify the key molecule or structure which is responsible for the water retaining capacity of normal uninjured cartilage and why the TEC-mediated repair tissue is compromised in this regard.

Despite the differences in the structure and permeability between the superficial zone of the uninjured and the TEC-mediated repair cartilage, no statistically significant differences were observed in the coefficient of friction. The coefficient of friction is known to strongly depend on interstitial fluid pressurisation (Ateshian *et al.*, 2009). Given the higher permeability of the superficial zone, a diminished ability to maintain fluid load support in the TEC group was expected, translating into an increase in the measured coefficient of friction. This, however, was not observed in the present study. There are likely two points contributing to such discrepancy. First, the coefficient of friction was measured 60 s after the application of normal load, when the boundary lubrication became dominant. At that moment, the boundary film on the cartilage surface, such as lipid and protein, likely played a major role in lubrication and thus, the effect of interstitial fluid pressure may have been diminished. Secondly, even if the effect of interstitial fluid pressure remained, the modulus of the repair cartilage became softer than normal cartilage while the permeability became greater at the surface.

One of the limitations of this study was that it followed the results up to only 6 months after surgery and it is not clear whether the findings observed in the present study would continue over the long-term, or improve with time post-implantation. Specifically, there may be the possibility for the further improvement of the structure of the superficial tangential zone and of the corresponding mechanical properties of the TEC-mediated repair tissue. Longer follow up studies will be required. The use of immature pigs might be another concern. However, we had previously confirmed that skeletal maturity does not affect the quality of the TEC-mediated repair cartilage, using the same surgical model (Shimomura *et al.*, 2010), and thus the use of immature animals has been somewhat validated. Another limitation was using uninjured specimens from the same condyle which had undergone surgery. Even "uninjured" articular surfaces may have been influenced by inflammatory responses following implantation, as well as the mechanical effect of incongruence created by those chondral defects. Therefore, these specimens might not be the most perfect "normal" control. However, extensive morphological analyses showed that the uninjured cartilage showed exactly the features as normal cartilage. Finally, we failed to directly prove the structure-function relationship in the articular surface due to the missing sample to sample correspondence between the histological scoring and biomechanical testing, and, therefore, direct statistical correlations could not be calculated. However, the significant inferiority in histological scores of the superficial zone of the TEC-mediated repair cartilage compared to the uninjured cartilage, as well as the significantly inferior biomechanical properties – including micro-scale stiffness and permeability in the superficial zone of the TEC-treated tissue to the uninjured cartilage – strongly suggest correlations between the microscopic structural features, with the altered micro-biomechanical properties in the articular surface, do exist.

This study revealed unique structural abnormalities in the superficial zone of the TEC-mediated cartilaginous repair tissue. Although not discussed widely, a critical review of publications focused on cell-based cartilage repair suggests that the predominance of fibro-cartilaginous tissue at the superficial zone of the repair cartilage was likely not peculiar to the present study, but was rather commonly observed in cell-based cartilage repair using autologous chondrocytes and MSCs (Knutsen *et al.*, 2004; Saris *et al.*, 2008; Gooding *et al.*, 2006; Nejadnik *et al.*, 2010). It is our speculation that it is not likely to develop functional articular surface structure by the implantation of a biomechanically immature implant without any follow-up treatment. In this regard, the restoration of the lamina splendens and the superficial tangential zone, which is the specialised membrane-like structure composed of densely packed collagen fibrils, should be an important target to focus on for the improvement of cartilage repair quality as the field moves towards tissue regeneration.

Conclusions

Cartilage defects, repaired by implantation of a scaffold-free tissue engineered construct (TEC) derived from synovial mesenchymal stem cells, are cartilaginous tissue which exhibited macro-scale compressive properties similar to uninjured cartilage. However, the TEC-mediated repair cartilage lacks the lamina splendens, as well as the superficial tangential zone, and exhibits inferior micro-scaled mechanical properties such as surface stiffness and water retaining capacity. Further improvement of these surface structures will be required to optimise cartilage regeneration.

Acknowledgements

We thank Dr. Daisuke Katakai, Miss Machiko Imura and Takuya Suzuki for assistance with the AFM and Micro-indentation testing as well as Dr. Kosuke Tateishi for animal surgery. We also appreciate the generosity of Dr John Sandy (Rush University, Chicago, IL, USA) for providing the antibody against PRG4 The present study was financially supported in part by the NEDO (Three-dimensional Complex Organ Structure project) (06001904-0), and the MEXT (BERC, Kogakuin University).

References

Ando W, Tateishi K, Hart DA, Katakai D, Tanaka,Y, Nakata K, Hashimoto J, Fujie H, Shino K, Yoshikawa H, Nakamura N (2007) Cartilage repair using an *in vitro* generated scaffold-free tissue-engineered construct derived from porcine synovial mesenchymal stem cells. Biomaterials **28**: 5462-5470.

Ando W, Tateishi K, Katakai D, Hart DA, Higuchi C, Nakata K, Hashimoto J, Fujie H, Shino K, Yoshikawa H, Nakamura N (2008) *In vitro* generation of a scaffold-free tissue-engineered construct (TEC) derived from human synovial mesenchymal stem cells: biological and mechanical properties and further chondrogenic potential. Tissue Eng Part A **14**: 2041-2049.

Ateshian GA (2009) The role of interstitial fluid pressurization in articular cartilage lubrication. J Biomech **42**: 1163-1176.

Buckwalter JA (2002) Articular cartilage injuries. Clin Orthop Relat Res **402**: 21-37.

De Bari C, Dell'Accio F, Tylzanowski P, Luyten FP (2001) Multipotent mesenchymal stem cells from adult human synovial membrane. Arthritis Rheum **44**: 1928-1942.

Dunham J, Shackleton DR, Billingham ME, Bitensky L, Chayen J, Muir IH (1988) A reappraisal of the structure of normal canine articular cartilage. J Anat **157**: 89-99.

Fujie H, Suzuki T, Katakai D, Ando W, Nakamura N (2007) Atomic force microscopic study on micro-compressive properties of cartilage repaired with scaffold-free three-dimensional bioengineered tissues (3DSTs), Proc 6th Comb Meet Orthopaed Res Soc, 37.

Gooding CR, Bartlett W, Bentley G, Skinner JA, Carrington R, Flanagan A (2006) A prospective, randomised study comparing two techniques of autologous chondrocyte_implantation for osteochondral defects in the knee: Periosteum covered *versus* type I/III collagen covered. Knee **13**: 203-210.

Grad S, Loparic M, Peter R, Stolz M, Aebi U, Alini M (2012) Sliding motion modulates stiffness and friction coefficient at the surface of tissue engineered cartilage. Osteoarthritis Cartilage, in press.

Hollander AP, Dickinson SC, Kafienah W (2010) Stem cells and cartilage development: complexities of a simple tissue. Stem Cells **28**: 1992-1996.

Hsieh CH, Lin YH, Lin S, Tsai-Wu JJ, Herbert Wu CH, Jiang CC (2008) Surface ultrastructure and mechanical property of human chondrocyte revealed by atomic force microscopy. Osteoarthritis Cartilage **16**: 480-488.

Hunziker EB (2002) Articular cartilage repair: basic science and clinical progress. A review of the current status and prospects. Osteoarthritis Cartilage **10**: 432-463.

Jankowski RJ, Deasy BM, Huard J (2002) Muscle-derived stem cells. Gene Ther **9**: 642-647.

Jay GD (1992) Characterization of a bovine synovial fluid lubricating factor. I. Chemical, surface activity and lubricating properties. Connect Tissue Res **28**: 71-88.

Katakai D (2008) Biomechanics of cartilage repair using mesenchymal stem cells. Ph.D. Dissertation (Kogakuin University).

Katakai D, Imura M, Ando W, Tateishi K, Yoshikawa H, Nakamura N Fujie H (2009) Compressive properties of cartilage-like tissues repaired *in vivo* with scaffold-free, tissue engineered constructs. Clin Biomechanics **24**: 110-116.

Knutsen G, Engebretsen L, Ludvigsen TC, Drogset JO, Grøntvedt T, Solheim E, Strand T, Roberts S, Isaksen V, Johansen O (2004) Autologous chondrocyte implantation compared with microfracture in the knee. A randomized trial. J Bone Joint Surg Am **86**: 455-464.

Koga H, Shimaya M, Muneta T, Nimura A, Morito T, Hayashi M, Suzuki S, Ju YJ, Mochizuki T, Sekiya I (2008) Local adherent technique for transplanting mesenchymal stem cells as a potential treatment of cartilage defect. Arthritis Res Ther **10**: R84.

Koga H, Engebretsen L, Brinchmann JE, Muneta T, Sekiya I (2009) Mesenchymal stem cell-based therapy for cartilage repair: a review. Knee Surg Sports Traumatol Arthrosc **17**: 1289-1297.

Kumar P, Oka M, Toguchida J, Kobayashi M, Uchida E, Nakamura T, Tanaka K (2001) Role of uppermost superficial layer of articular cartilage in the lubrication mechanism of joints, J Anat **199**: 241-250.

Lee OK, Kuo TK, Chen WM, Lee KD, Hsieh SL, Chen TH (2003) Isolation of multipotent mesenchymal stem cells from umbilical cord blood. Blood **103**: 1669-1675.

MacConaill MA (1951) The movements of bones and joints; the mechanical structure of articulating cartilage. J Bone Joint Surg Br **33**: 251-257.

Mansour JM, Mow VC (1976) The permeability of articular cartilage under compressive strain and at high pressures. J Bone Joint Surg Am **58**: 509-516.

Maroudas A, Bullough P, Swanson SA, Freeman MA (1968) The permeability of articular cartilage. J Bone Joint Surg Br **50**: 166-177.

Mow VC, Fithian DC, Kelly MA (1990) Fundamentals of articular cartilage and meniscus biomechanics. In: Articular Cartilage and Knee Joint Function: Basic Science and Arthroscopy (Ewing JW, ed), Raven Press, New York, pp 1-18.

Muir H, Bullough P, Maroudas A (1970) The distribution of collagen in human articular cartilage with some of its physiological implications. J Bone Joint Surg Br **52**: 554-563.

Nansai R, Suzuki T, Shimomura K, Ando W, Nakamura N, Fujie H (2011) Surface morphology and stiffness of cartilage-like tissue repaired with a scaffold-free tissue engineered construct. J Biomech Sci Eng**6**: 40-48.

Nejadnik H, Hui JH, Feng Choong EP, Tai BC, Lee EH (2010) Autologous bone marrow-derived mesenchymal stem cells *versus* autologous chondrocyte implantation: an observational cohort study. Am J Sports Med **38**: 1110-1116.

O'Driscoll SW, Keeley FW, Salter RB (1988) Durability of regenerated articular cartilage produced by free autogenous periosteal grafts in major full-thickness defects in joint surfaces under the influence of continuous passive motion. A follow-up report at one year. J Bone Joint Surg Am **70**: 595-606.

Pickard JE, Fisher J, Ingham E, Egan J (1998) Investigation into the effects of proteins and lipids on the frictional properties of articular cartilage. Biomaterials **19**: 1807-1812.

Pittenger MF, Mackay AM, Beck SC, Jaiswal RK, Douglas R, Mosca JD, Moorman MA, Simonetti DW, Craig S, Marshak DR (1999) Multilineage potential of adult human mesenchymal stem cells. Science **284**: 143-147.

Rieppo J, Hyttinen MM, Halmesmaki E, Ruotsalainen H, Vasara A, Kiviranta I, Jurvelin JS, Helminen HJ (2009) Changes in spatial collagen content and collagen network architecture in porcine articular cartilage during growth and maturation. Osteoarthritis Cartilage **17**: 448-455.

Sakaguchi Y, Sekiya I, Yagishita K, Muneta T (2005) Comparison of human stem cells derived from various mesenchymal tissues: superiority of synovium as a cell source. Arthritis Rheum **52**: 2521-2529.

Saris DB, Vanlauwe J, Victor J, Haspl M, Bohnsack M, Fortems Y, Vandekerckhove B, Almqvist KF, Claes T, Handelberg F, Lagae K, Van der Blauwhede J, Vandenneucker H, Yang KG, Jelic M, Verdonk R (2008) Characterized chondrocyte implantation results in better structural repair when treating symptomatic cartilage defects of the knee in a randomized controlled trial *versus* microfracture. Am J Sports Med **36**: 235-246.

Schmidt TA, Plaas AH, Sandy JD (2009) Disulfide-bonded multimers of proteoglycan 4 PRG4 are present in normal synovial fluids. Biochim Biophys Acta **1790**: 375-384.

Shimomura K, Ando W, Tateishi K, Nansai R, Fujie H, Hart DA, Kohda H, Kita K, Kanamoto T, Mae T, Nakata K, Shino K, Yoshikawa H, Nakamura N (2010) The influence of skeletal maturity on allogenic synovial mesenchymal stem cell-based repair of cartilage in a large animal model. Biomaterials **31**: 8004-8011.

Stolz M, Raiteri R, Daniels AU, VanLandingham MR, Baschong W, Aebi U (2004) Dynamic elastic modulus of porcine articular cartilage determined at two different levels of tissue organization by indentation-type atomic force microscopy. Biophys J **86**: 3269-3283.

Swann DA, Sotman S, Dixon M, Brooks C (1977) The isolation and partial characterization of the major glycoprotein (LGP-I) from the articular lubricating fraction from bovine synovial fluid. Biochem J **161**: 473-485.

Teshima R, Otsuka T, Takasu N, Yamagata N, Yamamoto K (1995) Structure of the most superficial layer of articular cartilage. J Bone Joint Surg Br **77**: 460-464.

Thambyah A, Broom N (2007) On how degeneration influences load-bearing in the cartilage-bone system: a microstructural and micromechanical study. Osteoarthritis Cartilage **15**: 1410-1423.

Weiss JA, Maakestad BJ (2006) Permeability of human medial collateral ligament in compression transverse to the collagen fiber direction. J Biomech **39**: 276-83.

Wickham MQ, Erickson GR, Gimble JM, Vail TP, Guilak F (2003) Multipotent stromal cells derived from the infrapatellar fat pad of the knee. Clin Orthop **412**: 196-212.

Discussion with Reviewers

Reviewer I: The presence and function of a distinct lamina splendens layer has been a somewhat controversial topic within the field of cartilage research. Here you suggest that this layer could be important for establishing the permeability and, thereby, the viscoelastic properties of the repair tissue. Does the literature suggest what sort of starting material might be placed in the defect to reconstitute the lamina splendens? Alternatively, do you think it would be feasible to reproduce this thin, acellular material *in vitro* and "coat" it onto a freshly-filled defect as a means to improve the immediate functionality of the repair?

Authors: As far as we can ascertain, there are unfortunately no reports in the available literature which address the reconstruction of the lamina splendens itself. Hollander *et al.* (2010; text reference) also emphasised the importance of regeneration of the lamina splendens at the joint surface. However, it may be a significant challenge to restore the integrity of the lamina splendens and future innovative studies are certainly needed to solve this problem. The suggestion of reproducing a thin, acellular material *in vitro* and "coating" it onto a freshly-filled defect is very interesting and worth trying for the immediate functional repair.

Reviewer II: This study follows on from previous studies conducted by this group, namely; Ando *et al.* (2007), Ando *et al.* (2008), Katakai *et al.* (2009) and Shimomura *et al.* (2010) (text references). These studies have explored the various properties of TEC derived from synovial mesenchymal stem cells in relation to biomechanics, tissue maturity, cartilage repair and chondrogenicity. Figures 1,

3 and 4 have appeared in subtly different forms in earlier manuscripts and essentially duplicate the results seen in these earlier manuscripts. The results of the macro-scale tangent modules (Fig. 3d) between Normal and TEC cartilage were reported in Fig. 5 of Ando *et al.* (2007), and the results of frictional coefficient also reported in the same Figure in the same manuscript for essentially the same experiment with different parameters. Please comment.

Reviewer V: Outcomes of a similar experiment were already reported in Ando *et al.* (2007), and are hence not real "novel" data. Similar data as presented in Fig. 3 was reported previously, as well (is Fig. 3D not based on the same data as Fig. 6B in Katakai *et al.*, 2009?). Please comment.

Authors: We used the same immature animals as in the previous studies of Ando *et al.* (2007) and Katakai *et al.* (2009) (text references). However, we have performed more detailed and different analysis, namely histological and micro-scaled biomechanical analysis of the surface structure of the repair cartilage. Although there are some similar data observed, analogous to the previous studies, such data have been used as the introduction of the new investigations conducted in the present study. Furthermore, even with regard to the somewhat similar data, the detailed experimental conditions of the mechanical analysis were quite different from the previous studies. The histological figures also have been obtained from different areas of the samples, something not done previously. Therefore, all data in this paper are not the simple reuse of those from the previous studies. We believe the inclusion of these data helps the readers to clearly understand the whole story of the present study (and why we focused on the analysis of details of the superficial structure).

Reviewer II: As PRG4 is a secreted protein most of antibody labelling is extracellular, therefore we are not able to observe if cells in the TEC are producing this protein. Following on from the latter point, it is well known that PRG4 from the synovium or surrounding cartilage that is secreted into the synovial fluid can be deposited onto surrounding (TEC) cartilage. Therefore, the presence of antibody labelling in TEC cartilage does not reveal anything conclusive about cellular production of PRG4 by differentiated MSCs in TEC cartilage. The authors' analysis of these observations is insufficient. Please comment.

Authors: Since the localisation of PRG4 (Lubricin) has been considered to be related to its tissue lubrication property, we investigated the localisation of PRG4 by immunohistochemical analysis as a potential indicator of tissue surface lubrication integrity. PRG4 was localised at the surface layer of normal cartilage, as well as the TEC-mediated repair cartilage. On the other hand, the purpose of PRG4 staining was not to detect the cellular source of the PRG4 but to assess the localisation of the PRG4 molecule at the superficial zone of repair tissue, which might be related to lubrication at the tissue surface. Therefore, we have decided not to add further analysis regarding the localisation of the cellular production of PRG4 (e.g., by *in situ* hybridisation) in the present study.

Reviewer III: The permeability of cartilage is known to be strain-dependant. The authors compressed their samples by 30 % prior to permeability testing. Please clarify the motivation for this.

Authors: To avoid leaking water, it was required to tighten the water pipe to the cartilage surface in the experiment. Therefore, the permeability test was performed at the compressive strain of 30 %. Using the equation for Darcy's law indicated in the text, it is possible to calculate the permeability at any strain.

Reviewer III: The micro-indentation testing revealed differences in the surface properties of normal and engineering tissues. This was not extended to testing deeper regions of the tissue. Would this be possible? Such analysis may reveal more subtitle difference in the mechanics of other regions of the repair tissue.

Authors: Unfortunately, we did not perform such an AFM measurement on the tissue although it should be possible to do in the future. In the future, we would like to perform the AFM measurement on each layer of uninjured cartilage and the repair tissue.

Reviewer IV: The authors describe positive staining for PRG4 to be in the surface (Fig. 7a). There appears to be some staining in/of the cells lower in the cartilage also, at least in the image from the untreated group. Do the authors have any comment on this?

Authors: The positive staining of PRG4 was observed in the image of the untreated defect group. It is well known that synovial cells synthesise PRG4 (Schumacher *et al.*, 1999, additional reference). We speculated that this fibrous tissue in the untreated group might have been developed by cells from the surrounding synovial tissues and thus express the PRG4. With this speculation, there may have been some positive staining detected in the deeper area due to infiltration of the defect by such cells.

Reviewer IV: How relevant do the authors think that an injury model in a 4 month old pig is to the reparative capacity of mature and ageing humans with degenerative musculoskeletal conditions?

Authors: We have previously confirmed the feasibility of the TEC to facilitate cartilage repair regardless of skeletal maturity (Shimomura *et al.*, 2010, text reference). Therefore, the factor of aging (maturity) could be of negligible influence on the outcome of treatment. In other words, the use of immature animal has been validated to have clinical relevance. We have currently no evidence regarding the effect of potential degenerative conditions on repair using a TEC approach. Clearly osteoarthritis is an inflammatory condition, so the point is relevant but answers must await results of future investigations.

Reviewer V: Can the shape and size of the TEC be controlled? This might be a necessary requirement for future application.

Authors: The size of the TECs can be controlled by changing the size of the culture dishes to be used and

cell number to be inoculated. Thus, we chose the most suitable size of culture dish for the present studies, as well as prepared the required number of cells based on the estimated volume of the cartilage lesions/defects which is measured macroscopically, arthroscopically, or by MRI before implantation surgery. Details can be found in Ando *et al.* (2007) and Ando *et al.* (2008) (text references).

Reviewer V: Why were the TECs prepared as allografts without chondrogenic stimulation? If the allografts were stimulated chondrogenically, would there still be such a difference in the biomechanical stability of the superficial layer?
Authors: We are currently investigating the implantation of the TEC with stimulation by relevant growth factors. We are interested in the potential improvement of the superficial zone by any biological manipulation of the TEC prior to or concurrent at the time of implantation. Hopefully, we will be able to report the results of such studies in the not so distant future.

Reviewer V: It would actually be quite interesting to also test the edges of the specimens, rather than only the centre for biomechanical stability, especially as this can be hugely important in preventing graft failure.
Authors: We have recently completed measurement of the integration strength of the implants, and the results are in preparation for a future submission. Interestingly, we have found that the integration strength also depends on the depth (deep lesion shows the highest strength and superficial shows the lowest value). However, some details remain to be confirmed, but we hope to be able to report the results in the near future.

Reviewer V: The introduction of depth dependent differences may well be very important for the successful long term performance of regenerative implants. Other cell sources, such as chondrocytes or bone marrow derived stem cells may, based on recent findings in the literature, be (more) suitable. Have the authors any experience with these in their model and/or could they hypothesise how these cells would be have in their approach?
Authors: The reason for the use of synovial MSCs is based on the reported characteristics of synovial MSCs such as the retention of multipotent differentiation potential over many passages of culture (De Bari *et al.*, 2001, text reference) and superior chondrogenic potential among MSCs derived from many tissues (Sakaguchi *et al.*, 2005, text reference). We have not had any experience with MSCs derived from other tissues; however, based on the cellular characteristics, we believe that the synovium could be one of the most suitable cell sources for cartilage regeneration therapies.

Reviewer VI: Can you explain the large degree of variability in the quasi-static compression testing, as reflected by the high coefficients of variance (= SD/mean)? Is such inter-sample variability typical for this sort of test?
Authors: Since the edge of the AFM probe is nano-scale and the indentation depth is less than micro-scale, the results of the indentation test are site-specific. Therefore, it is likely that the variability in the surface condition of tissue samples could potentially have led to the somewhat high inter-sample variability in the test. Perhaps with further time post-implantation some of this variability may disappear, but currently it is the "state of the art".

Additional Reference

Schumacher BL, Hughes CE, Kuettner KE, Caterson B, Aydelotte MB (1999) Immunodetection and partial cDNA sequence of the proteoglycan, superficial zone protein, synthesized by cells lining synovial joints. J Orthop Res **17**: 110-120.

PLoS one

Nkx3.2 Promotes Primary Chondrogenic Differentiation by Upregulating *Col2a1* Transcription

Yoshitaka Kawato[1], Makoto Hirao[2], Kosuke Ebina[1]*, Kenrin Shi[1], Jun Hashimoto[2], Yui Honjo[1], Hideki Yoshikawa[1], Akira Myoui[3]

1 Department of Orthopaedics, Graduate School of Medicine, Osaka University, Yamadaoka, Suita, Osaka, Japan, **2** Department of Orthopaedic Surgery, National Hospital Organization, Osaka Minami Medical Center, Kawachinagano, Osaka, Japan, **3** Medical Center for Translational Research, Osaka University Hospital, Yamadaoka, Suita, Osaka, Japan

Abstract

Background: The Nkx3.2 transcription factor promotes chondrogenesis by forming a positive regulatory loop with a crucial chondrogenic transcription factor, Sox9. Previous studies have indicated that factors other than Sox9 may promote chondrogenesis directly, but these factors have not been identified. Here, we test the hypothesis that Nkx3.2 promotes chondrogenesis directly by Sox9-independent mechanisms and indirectly by previously characterized Sox9-dependent mechanisms.

Methodology/Principal Findings: C3H10T1/2 pluripotent mesenchymal cells were cultured with bone morphogenetic protein 2 (BMP2) to induce endochondral ossification. Overexpression of wild-type Nkx3.2 (WT-Nkx3.2) upregulated glycosaminoglycan (GAG) production and expression of type II collagen α1 (*Col2a1*) mRNA, and these effects were evident before WT-Nkx3.2-mediated upregulation of *Sox9*. RNAi-mediated inhibition of *Nkx3.2* abolished GAG production and expression of *Col2a1* mRNA. Dual luciferase reporter assays revealed that WT-Nkx3.2 upregulated *Col2a1* enhancer activity in a dose-dependent manner in C3H10T1/2 cells and also in N1511 chondrocytes. In addition, WT-Nkx3.2 partially restored downregulation of GAG production, Col2 protein expression, and *Col2a1* mRNA expression induced by *Sox9* RNAi. ChIP assays revealed that Nkx3.2 bound to the *Col2a1* enhancer element.

Conclusions/Significance: Nkx3.2 promoted primary chondrogenesis by two mechanisms: Direct and Sox9-independent upregulation of *Col2a1* transcription and upregulation of *Sox9* mRNA expression under positive feedback system.

Citation: Kawato Y, Hirao M, Ebina K, Shi K, Hashimoto J, et al. (2012) Nkx3.2 Promotes Primary Chondrogenic Differentiation by Upregulating *Col2a1* Transcription. PLoS ONE 7(4): e34703. doi:10.1371/journal.pone.0034703

Editor: Antonio Moschetta, University of Bari & Consorzio Mario Negri Sud, Italy

Received November 25, 2011; **Accepted** March 5, 2012; **Published** April 12, 2012

Funding: This work was supported by grants from the Japan Science and Technology Agency. The funder had no role in study design, data collection and analysis, decision to publish, or preparation of the manuscript.

Competing Interests: The authors have declared that no competing interests exist.

* E-mail: k-ebina@umin.ac.jp

Introduction

During endochondral ossification, chondrogenesis is executed in multiple steps [1]. In the early steps of chondrogenesis, the Sox9 transcription factor is a crucial inducer of the expression of chondrocyte-specific genes [2,3]. However, the latter steps of chondrogenesis are regulated by Runx-family transcription factors [4,5]. We recently reported that hypoxia (5% oxygen tension) promotes chondrogenesis and glycosaminoglycan (GAG) production and that it suppresses hypertrophy of chondrocytes and osteoblastic differentiation in C3H10T1/2 cell culture [6]. Nkx3.2 (also known as Bapx1), a member of the NK homeobox gene family, is a transcriptional repressor that regulates Runt related transcription factor 2 (Runx2) expression as part of a tight positive regulatory system that includes Sox9; this system is initiated by Sonic hedgehog (Shh) [7,8,9,10]. Lassar's group demonstrated that Nkx3.2 also promotes primary chondrogenic differentiation using primary presomitic mesodermal explants [7], but a direct, Sox9-independent relationship between Nkx3.2 and type II collagen α1 (Col2a1), a marker of primary chondrogenic differentiation, has not been reported.

In humans, a rare form of skeletal dysplasia, called spondylomegaepiphysial-metaphysial dysplasia (SMMD), is caused by homozygous inactivating mutations in the *NKX3.2* gene [11]. The skeletal phenotypes seen in SMMD patients are morphologically similar to those observed in *Nkx3.2* null mice [12]. The human and mouse *Nkx3.2* mutations are associated not only with severe dysplasia of vertebral column, but also arrested development of intervertebral discs, which is similar to that seen in *Col2a1* null mice [13]. Therefore, we hypothesized that there must be a Sox9-independent mechanism for Nkx3.2 to promote primary chondorogenesis by activating *Col2a1* transcription.

Here, we used the C3H10T1/2 pluripotent mesenchymal cell line and the N1511 murine chondrocyte cell line and demonstrated that Nkx3.2 promotes primary chondrogenesis during endochondral ossification by directly activating *Col2a1* transcription.

Materials and Methods

Cell Culture and Analysis for Chondrogenic Differentiation

C3HT101/2 cells were purchased from RIKEN Bio-Resource Center (Saitama, Japan) and were cultured in Dulbecco's modified Eagle's medium (Invitrogen, San Diego, CA). The N1511 murine chondrocyte cell line [14], which was kindly donated by Dr. Hideto Watanabe and Dr. Nobuhiro Kamiya, was also cultured in Dulbecco's modified Eagle's medium. When cultures were approximately 90% confluent, recombinant human bone morphogenic protein 2 (rh-BMP2), which was donated by Osteopharma Inc. (Osaka, Japan), was added to stimulate chondrogenesis. To evaluate chondrogenic differentiation, C3H10T1/2 cells were fixed with 10% formalin and then washed with 0.1N HCl in distilled water; washed cells were stained for 60 min with alcian blue solution, alcian blue 8GX (Sigma, St. Louis, MO) and rinsed twice with 0.1 N HCl to remove any unbound dye. To quantify GAG synthesis, alcian blue is extracted by 4 M guanidine-HCl overnight at 4°C. Absorbance values are read at 600 nm after temperature equilibration.

Proliferation assay

C3H10T1/2 cells were cultured in 96-well plates at a concentration of 1.0×10^4 cells/cm^2, and they were stimulated with rh-BMP2 (300 ng/ml). Cell proliferation was assessed using the Cell Counting Kit-8 assay system (Dojindo, Kumamoto, Japan), according to the manufacturer's instructions.

Western blot analysis

Western blot analyses were performed using whole cell lysates. For the blots, 20 μg of each sample was applied. The blots were first incubated with anti-mouse collagen II antibodies (R&D Systems Inc., Minneapolis, MN) and then with horseradish peroxidase-conjugated anti- sheep IgG antibodies (R&D Systems Inc., Minneapolis, MN). Anti-mouse β-actin rabbit antibodies and horseradish peroxidase-conjugated anti-rabbit IgG antibodies were purchased from Cell Signaling Technology (Tokyo, Japan).

RNA interference and overexpression of *Nkx3.2* and *Sox9*

Commercially synthesized small interfering RNA (siRNA) and manufacturer's protocols were used for the RNAi experiments (B-Bridge International, Inc., Cupertino, CA). The sequences of sense strands of siRNA targeting *Nkx3.2* and *Sox9* mRNA and that of the negative control siRNA are shown in Table 1. The wild-type Sox9 (WT-Sox9) construct was donated by the Department of Biochemistry, Osaka University Graduate School, Faculty of Dentistry. The wild-type Nkx3.2 (WT-Nkx3.2) plasmid was constructed by inserting a full-length *Nkx3.2* cDNA into the pBApo-CMV Neo vector purchased from Takara Bio Inc., Otsu, Japan. When cultures were approximately 70% confluent, 10 nM of Nkx3.2 or Sox9 siRNA were transfected with 10 μM Lipofectamine RNAiMAX (Invitrogen). After 24-h transfection, MOCK plasmid or WT-Nkx3.2/Sox9 was transiently transfected by using FuGENE®6 transfection reagent (Roche, Indianapolis, IN) according to the manufacture's recommendation. After another 24-h culture (day 0), cells were continuously stimulated with BMP-2 (300 ng/ml) and cultured with the medium change at 3 days intervals.

Reporter Constructs and Luciferase Reporter Assay

Four tandem copies of a 48-bp chondrocyte-specific enhancer segment from the *type II collagen α1* (*Col2a1*) gene were synthesized as previously reported [15] and inserted into the pGL3-Promoter vector (Promega, Madison, WI); this construct was designated 4Col2E-Luc. A GTGAAT motif was deleted from this 48-bp enhancer segment to generate a 42-bp segment; an array of four tandem copies of this 42-bp segment was synthesized and inserted into the pGL3-Promoter vector purchased from UNITECH (Chiba, Japan). This construct was designated D4Col2E-Luc. In reporter assays, cells were transiently transfected with 0.4 μg of the 4Col2E-Luc or the D4Col2E-Luc construct and 0.01 μg of the TK-Renilla luciferase construct (TK *Renilla*) (Promega). Luciferase activity was measured using a Dual Luciferase assay kit (Promega) and luminometer (Berthold Technologies, Bad Wildbad, Germany), and reporter construct activity was normalized by comparison with activity from the *Renilla* luciferase construct. All experiments were performed in triplicate.

Table 1. Sequences of sense strands of siRNA targeting *Nkx3.2*, *Sox9* mRNA and of siRNA control.

Target gene	Oligonucleotide	Sequence (5′→3′)
Negative control	Sense	ATCCGCGCGATAGTACGTA
Nkx3.2	Sense	CCAAGGACCUGGAGGAGGATT
Sox9	Sense	GCCAGGUGCUGAAGGGCUATT

doi:10.1371/journal.pone.0034703.t001

Chromatin immunoprecipitation (ChIP)

Chromatin immunoprecipitation (ChIP) was performed using an EZ ChIP kit (Millipore, Billerica, MA). Anti-Nkx3.2 mouse antibodies, anti-Sox9 mouse antibodies, and normal rabbit immunoglobulin G (IgG) were all purchased from Santa Cruz Biotechnology, Inc. (Santa Cruz, CA). Qualitative PCR conditions were as follows: 1 cycle at 95°C for 2 min; 35 cycles at 95°C for 30 s, 60°C for 30 min, and 72°C for 30 min; and 1 cycle at 72°C for 7 min. Products were electrophoresed on a 3% agarose gel. ChIP primers targeting the *Col2a1* enhancer are shown in Table 2.

Standard and Quantitative RT-PCR

First-strand cDNA was synthesized using SuperScript III RNase H® reverse transcriptase (Invitrogen). Standard RT-PCR was performed using Ex Taq (Takara Bio Inc.). Quantitative RT-PCR was performed using the Roche Applied Science Light Cycler system. The SYBR Green assay, with which each cDNA sample was evaluated in triplicate 20-μl reactions, was used for all target transcripts. Expression values were normalized to *GAPDH* expression. The sequence of the primers used for standard and quantitative RT-PCR assays, are shown in Table 3.

Statistical analysis

All data are expressed as the mean ± standard deviation (SD) of a minimum of three replicate measurements. Differences between

Table 2. Primer sequences used in ChIP analysis of the *Col2a1* enhancer.

Primer	Sequence (5′→3′)
Forward	GGGAGACCTCAGTCCTCCTT
Reverse	AGAAAGGAGCCAACGCTGTA

doi:10.1371/journal.pone.0034703.t002

Table 3. Primer sequences used in PCR assays.

gene	Primer	Sequence (5′→3′)
Nkx3.2	Forward	AACCATCAGCGCTACCTGTC
	Reverse	CTTTACGGCCACTTTCTTGG
Col2a1	Forward	CCTGTCTGCTTCTTGTAAAAC
	Reverse	AAAAAATACAGAGGTGTTTGACACAGA
Sox9	Forward	ATGAATCTCCTGGACCCCTT
	Reverse	AACTTTGCCAGCTTGCACGT
Runx2	Forward	GCTTGATGACTCTAAACCTA
	Reverse	AAAAAGGGCCCAGTTCTGAA
GAPDH	Forward	TGAACGGGAAGCTCACTGG
	Reverse	TCCACCACCCTGTTGCTGTA

doi:10.1371/journal.pone.0034703.t003

groups were assessed using the ANOVA test. Any P value$<$0.05 was considered statistically significant.

Results

Overexpression of Nkx3.2 promotes and inhibition of *Nkx3.2* suppresses chondrogenic differentiation and GAG production in C3H10T1/2 cell culture

On days 5, 7, and 10, GAG production was higher in C3H10T1/2 cells overexpressing Nkx3.2 than in control cells (Fig. 1a, b). Expression of *Col2a1* mRNA was upregulated on days 5 and 7, and *Runx2* mRNA was downregulated on days 5, 7, and 10 in cells overexpressing Nkx3.2. However, *Sox9* expression was not upregulated until day 7 (Fig. 2a, b). Overexpression of Nkx3.2 upregulated cell proliferation in C3H10T1/2 cells on day 2, but no differences in cell proliferation were observed between control cells and overexpressing cells after day 5 (Fig. 1c). Inhibition of *Nkx3.2* using RNAi clearly suppressed GAG production on days 5, 7 and 10 (Fig. 1d, e) and expression of *Col2a1, and Sox9* mRNA, while upregulated *Runx2* expression on days 2, 5, and 7 (Fig. 2c, d). Inhibition of *Nkx3.2* downregulated the proliferation of C3H10T1/2 cells on day 2, but no differences in cell proliferation were observed after day 5 (Fig. 1f).

Nkx3.2 binds to the 48-bp chondrocyte-specific enhancer segments of *Col2a1* and upregulates *Col2a1* transcription

To assess the effects of Nkx3.2 on *Col2a1* enhancer activity, we performed a dual luciferase activity assay. The D4Col2E-Luc construct carried a deleted version of the enhancer carried in the 4Col2E-Luc construct; specifically, the enhance repeats in D4Col2E-Luc lack a GTGAAT motif (Fig. 3). WT-Nkx3.2 upregulated *Col2a1* enhancer activity in a dose-dependent manner (Fig. 4a). Next, we compared the activity from the 4Col2E-Luc and D4Col2E-Luc constructs in the presence of WT-Nkx3.2 or WT-Sox9 (Fig. 4b, c). Both WT-Nkx3.2 and WT-Sox9 clearly upregulated the transcriptional activity of 4Col2E-Luc (Fig. 4b). Moreover, WT-Nkx3.2 upregulated transcriptional activity of 4Col2E-Luc not only in C3H10T1/2 cells but also in N1511 chondrocytes (Fig. 4c). In contrast, WT-Nkx3.2 did not upregulate activity of the D4Col2E-Luc construct (Fig. 4b, c). We also used the ChIP assay to determine whether Nkx3.2 bound to the 48 bp *Col2a1* enhancer element, and found that Nkx3.2 did bind to this enhancer element (Fig. 4d).

Overexpression of Nkx3.2 partially restored downregulation of GAG production, Col2 protein expression, *and Col2a1* mRNA expression induced by si-*Sox9*

To assess Sox9-independent upregulation of *Col2a1* trascription by Nkx3.2, we performed *Sox9* inhibiting experiments using RNAi. On days 5, 7, and 10, GAG production was downregulated by si-*Sox9* compared to si-control (Fig. 5a). Si-*Sox9* downregulated *Col2a1* mRNA expression from day 2 and *Sox9* mRNA expression from day 0, while *Sox9* mRNA was restored on day 10 (Fig. 5c). Overexpression of Nkx3.2 upregulated its mRNA expression from day 0 to day 10, and partially restored downregulation of GAG production and Col2 protein expression induced by si-*Sox9* (Fig. 5a, b). Overexpression of Nkx3.2 with si-*Sox9* upregulated *Col2a1* mRNA expression even more than that of si-control+MOCK, and also tended to restore *Sox9* mRNA expression downregulated by si-*Sox9* suggesting positive feedback of Nkx3.2 to Sox9 (Fig. 5c).

Discussion

Previously, we presented the hypothesis that factors other than Sox9 directly promote chondrogenic differentiation [6]. Here, we tested our hypothesis by assessing whether Nkx3.2, a well-known transcriptional repressor of *Runx2*, directly regulates *Col2a1*, a marker of chondrogenesis [8,16].

Downregulation of *Nkx3.2* in mouse embryos results in severe skeletal dysplasia and death [10]. Interestingly, arrested development of the intervertebral discs in *Nkx3.2* null mice [12] is clearly reminiscent of the defects observed in *Col2a1* null mice [12]. These findings led us to suppose that *Nkx3.2* may play a crucial role in the regulation of *Col2a1* expression.

Previously, it has been reported that *Nkx3.2* gene expression begins somewhat earlier than *Sox9* expression during chondrogenic differentiation in C3H10T1/2 cells [8]. Here, we found that exogenous Nkx3.2-mediated upregulation of a chondrogenic gene, *Col2a1*, occurred earlier than Nkx3.2-mediated upregulation of *Sox9* (Fig. 2a, b). In addition, overexpression of Nkx3.2 partially restored downregulation of GAG production, Col2 protein expression, *and Col2a1* mRNA expression induced by si-*Sox9*, suggesting Sox9-independent mechanism for upregulation of *Col2a1* trascription by Nkx3.2.

Nkx3.2 reportedly binds to a HRAGTG motif [17]. Notably, we discovered a GTGAAT motif in the *Col2a1* enhancer element, and GTGAAT is the reverse of HRAGTG. Therefore, we speculated that Nkx3.2 may bind this reverse motif and regulate *Col2a1* transcription. We assessed the effects of overexpression of Nkx3.2 or Sox9 on *Col2a1* enhancer activity using the 4Col2E-Luc and D4Col2E-Luc constructs. These assays clearly demonstrated that Nkx3.2 overexpression upregulated 4Col2E-Luc activity, but Nkx3.2 overexpression had less of an effect than Sox9 overexpression. In addition, D4Col2E-Luc transcriptional activity was not upregulated by WT-Nkx3.2 overexpression, but WT-Sox9 overexpression resulted in upregulation of D4Col2E-Luc. We suppose that WT-Sox9 was able to upregulate D4Col2E-Luc because the 42-bp repeats in D4Col2E-Luc each contained three Sox-9 binding sites [15,18]. Taken together, these results indicate that the GTGAAT motif in the 48-bp *Col2a1* enhancer was important for the transcriptional activation mediated by either Nkx3.2 or Sox9. Finally, results of ChIP assays confirmed that Nkx3.2 did bind to the 48-bp *Col2a1* enhancer.

Reportedly, a trio of Sox proteins (Sox9, L-Sox5, and Sox6) is crucial to upregulation of *Col2a1* transcription [18]. However, Sox9-dependent transcriptional regulation in chondrogenesis requires cofactors in addition to these Sox proteins, such as

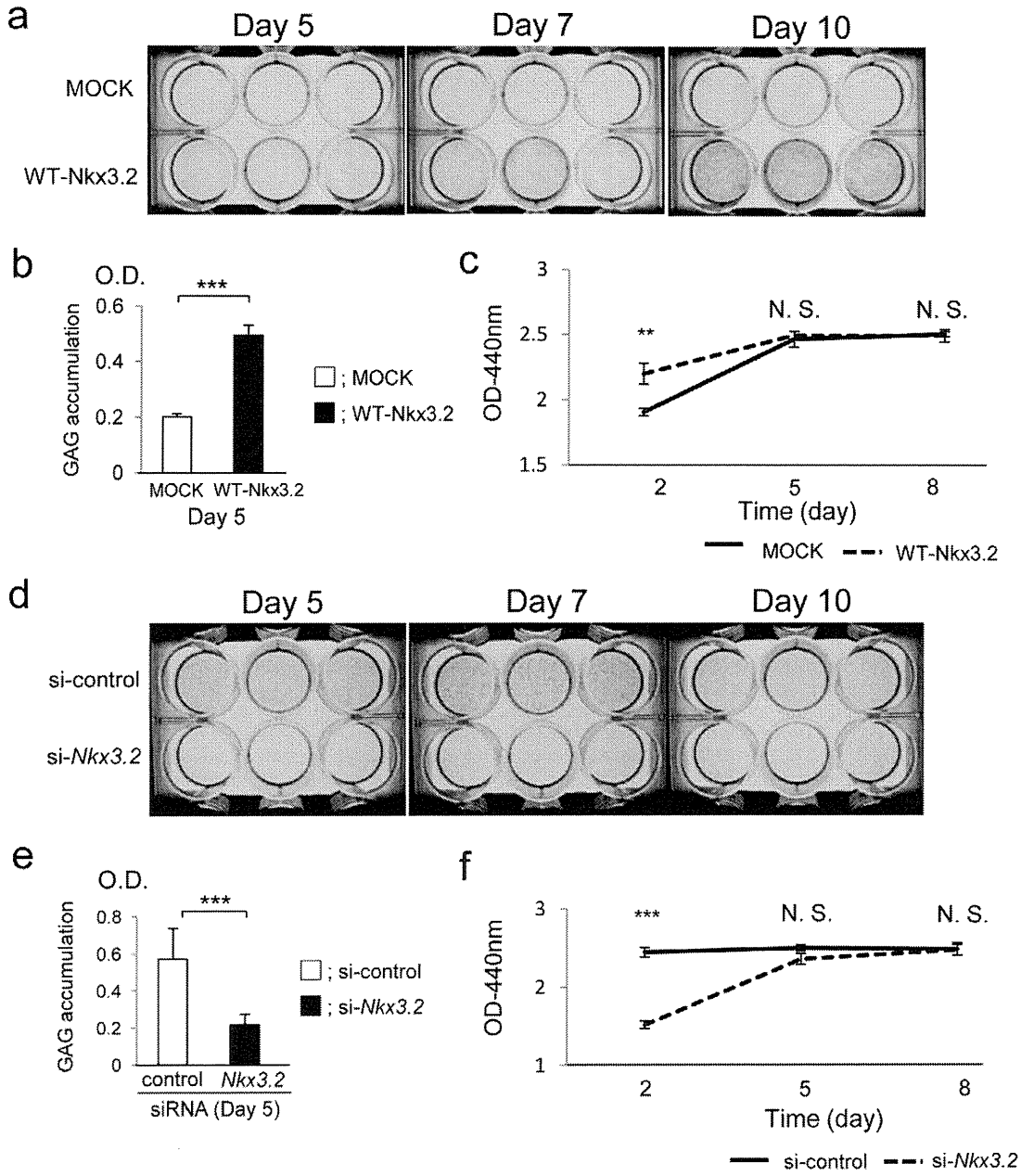

Figure 1. Overexpression of Nkx3.2 and inhibition of *Nkx3.2* affected GAG production and cell proliferation in C3H10T1/2 cell culture. a After 24-h transfection with MOCK plasmid (upper wells) or WT-Nkx3.2 (lower wells) (day 0), C3H10T1/2 cells were stimulated with BMP-2 (300 ng/ml) for 5, 7, or 10 days. At each time point, cells were stained with alcian blue. **b** Quantification of GAG synthesis by C3H10T1/2 cells on day 5. Data are shown as mean ± S.D. (n = 3). ***$P<0.001$. **c** Proliferation of C3H10T1/2 cells transfected with MOCK or WT-Nkx3.2 plasmid. Transfected C3H10T1/2 cells were stimulated with BMP-2 (300 ng/ml) for 8 days. Cell proliferation was assayed on day 2, 5, and 8. **$P<0.01$; *N.S.*, not significant. **d** After a 48-h transfection with negative control siRNA (upper wells) or with *Nkx3.2* siRNA (lower wells) (day 0), C3H10T1/2 cells were stimulated with BMP-2 (300 ng/ml) for 5, 7, or 10 days. At each time point, cells were stained with alcian blue. **e** Quantification of GAG synthesis by C3H10T1/2 cells on day 5. Data are means ± S.D. (n = 3). ***$P<0.001$. **f** Proliferation of C3H10T1/2 cells transfected with si-control or si-*Nkx3.2*. Transfected C3H10T1/2 cells were stimulated with BMP-2 (300 ng/ml) for 8 days. Cell proliferation was assayed on days 2, 5, and 8. ***$P<0.001$; *N.S.*, not significant.
doi:10.1371/journal.pone.0034703.g001

p300/CREB-binding protein (CBP), peroxisome proliferator-activated receptor γ (PPAR-γ) coactivator-1α (PGC-1α), and Smad3 [19,20,21,22,23]. Therefore, we first assumed that Nkx3.2 and some Sox family proteins cooperate to upregulate *Col2a1* enhancer activity. Meanwhile, our preliminary experiment showed that overexpression of Nkx3.2 and Sox9 together was more effective than overexpression of Nkx3.2 alone, but less effective than overexpression of Sox9 alone, in upregulating *Col2a1* enhancer activity (data not shown). Finally, exogenous Nkx3.2 partially restored GAG production, Col2 protein expression, *and Col2a1* mRNA expression downregulated by si-*Sox9*. Meanwhile, exogenous Nkx3.2 also tended to restore Sox9 after day 2, and this positive feedback may partially contribute to the restoration of GAG production and *Col2a1* mRNA expression by Sox9-dependent pathway. To obtain stronger downregulation of Sox9, we performed higher dose of si-*Sox9* experiments, which resulted

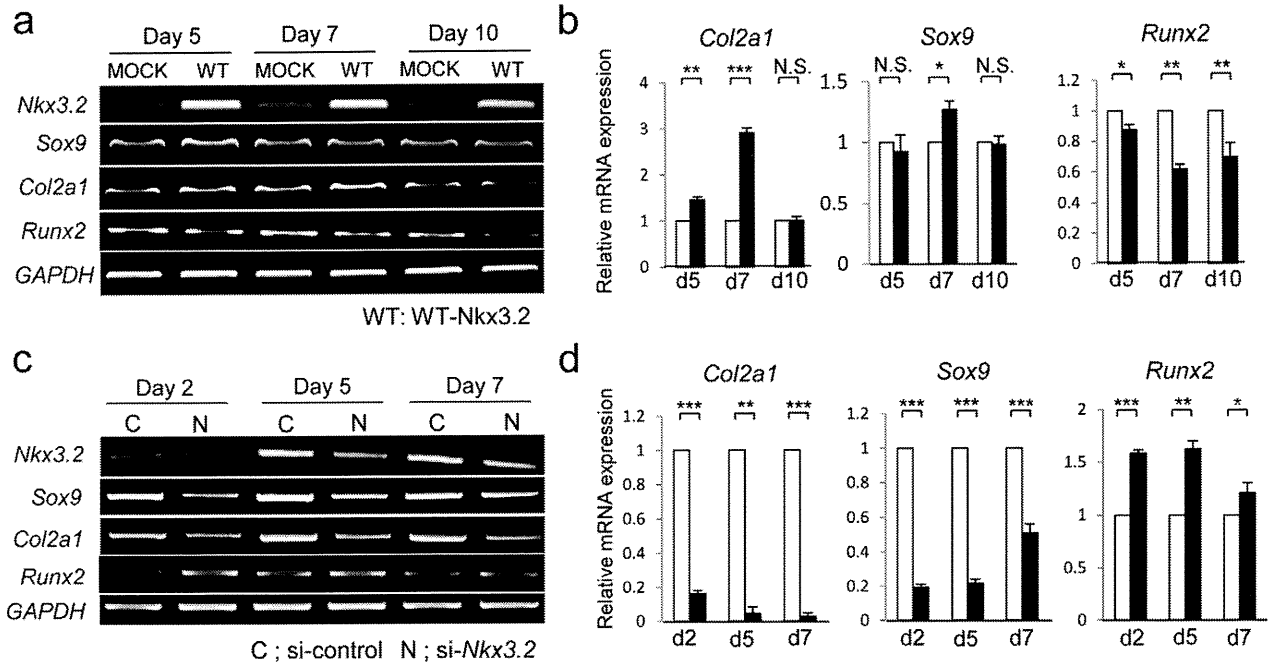

Figure 2. Overexpression of Nkx3.2 and inhibition of *Nkx3.2* affected mRNA expression of chondrogenic differentiation markers in C3H10T1/2 cell culture. a After 24-h transfection with MOCK plasmid or WT-Nkx3.2, C3H10T1/2 cells were stimulated with BMP-2 (300 ng/ml) for 5, 7, and 10 days and total RNA was extracted at each time point. RT-PCR was used to assess *Nkx3.2*, *Sox9*, *Col2a1*, *Runx2*, and *GAPDH* mRNA expression. **b** Real-time PCR for *Col2a1*, *Sox9*, *Runx2*, and *GAPDH* mRNAs were also performed. Values are normalized to the level of *GAPDH* mRNA. Data are presented as means ± S.D. (n = 3). **P*<0.05; ***P*<0.01; ****P*<0.001; *N.S.*, not significant. **c** After a 48-h transfection with negative control siRNA or with *Nkx3.2* siRNA (day 0), C3H10T1/2 cells were stimulated with BMP-2 (300 ng/ml) for 2, 5, and 7days. At each time point, total RNA was extracted. RT-PCR was used to assess *Nkx3.2*, *Sox9*, *Col2a1*, *Runx2*, and *GAPDH* mRNA expression. **d** Real-time PCR was also used to assess *Col2a1*, *Sox9*, *Runx2*, and *GAPDH* mRNA expression. Values are normalized to the level of *GAPDH* mRNA. Data are presented as means ± S.D. (n = 3). **P*<0.05; ***P*<0.01; ****P*<0.001.
doi:10.1371/journal.pone.0034703.g002

in decreased cell viability of C3H10T1/2 cells. Based on these findings, it seemed that Nkx3.2 could induce chondrogenesis by Sox9-independent mechanisms in C3H10T1/2 cells, but that it was less effective than Sox9.

Nkx3.2 expression is maintained in proliferative chondrocytes, and Nkx3.2 promotes viability of these cells by constitutively activating RelA during endochondral ossification [24]. Therefore, we first assumed that Nkx3.2 also controls the viability of C3H10T1/2 cells stimulated with BMP2. As shown in Fig. 1c and Fig. 1f, overexpression of Nkx3.2 upregulated and inhibition of *Nkx3.2* downregulated C3H10T1/2 cell proliferation on day 2, but there was no significant difference from days 5 to 8. Our quantitative RT-PCR data showed that expression of *type X collagen α1 (Col10a1)*, a hypertrophic chondrocyte marker, was detected from day 5 (data not shown). Although it is difficult to demonstrate that the phenotype of C3H10T1/2 cells stimulated with BMP2 for 2 days is similar to that of proliferative chondrocyte, it is plausible that Nkx3.2 affected cell proliferation in proliferative chondrocyte, while its effect seemed to vanish in hypertrophic chondrocytes.

This study has several limitations. We used only two cell lines in this study; therefore, we must investigate the interactions between Nkx3.2 and Col2a1 transcription in primary cell culture in future studies. In addition, we attempted to detect direct binding of Nkx3.2 to the 48-bp *Col2a1* enhancer using electrophoresis

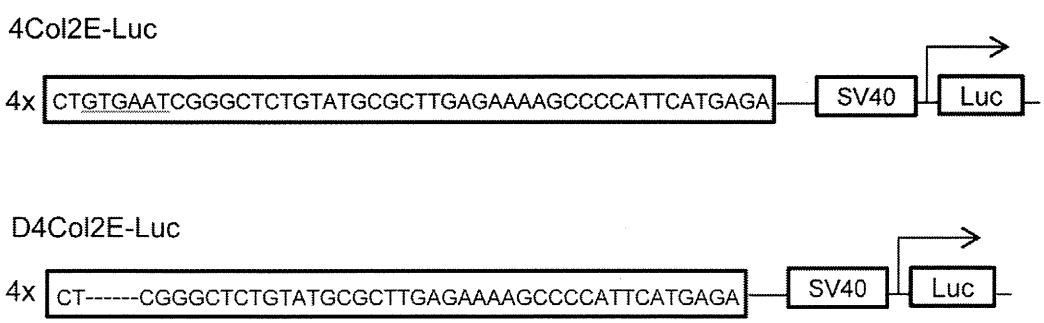

Figure 3. Schematic of reporter constructs. 4Col2E-Luc has four tandem copies of a 48-bp chondrocyte-specific enhancer segment from the *type II collagen α1* (*Col2a1*) gene. D4Col2E-Luc construct has four tandem copies of a 42-bp version of the 48-bp segment; a GTGAAT motif was deleted from the 48-bp chondrocyte-specific enhancer segment from *Col2a1* to generate the 42-bp version.
doi:10.1371/journal.pone.0034703.g003

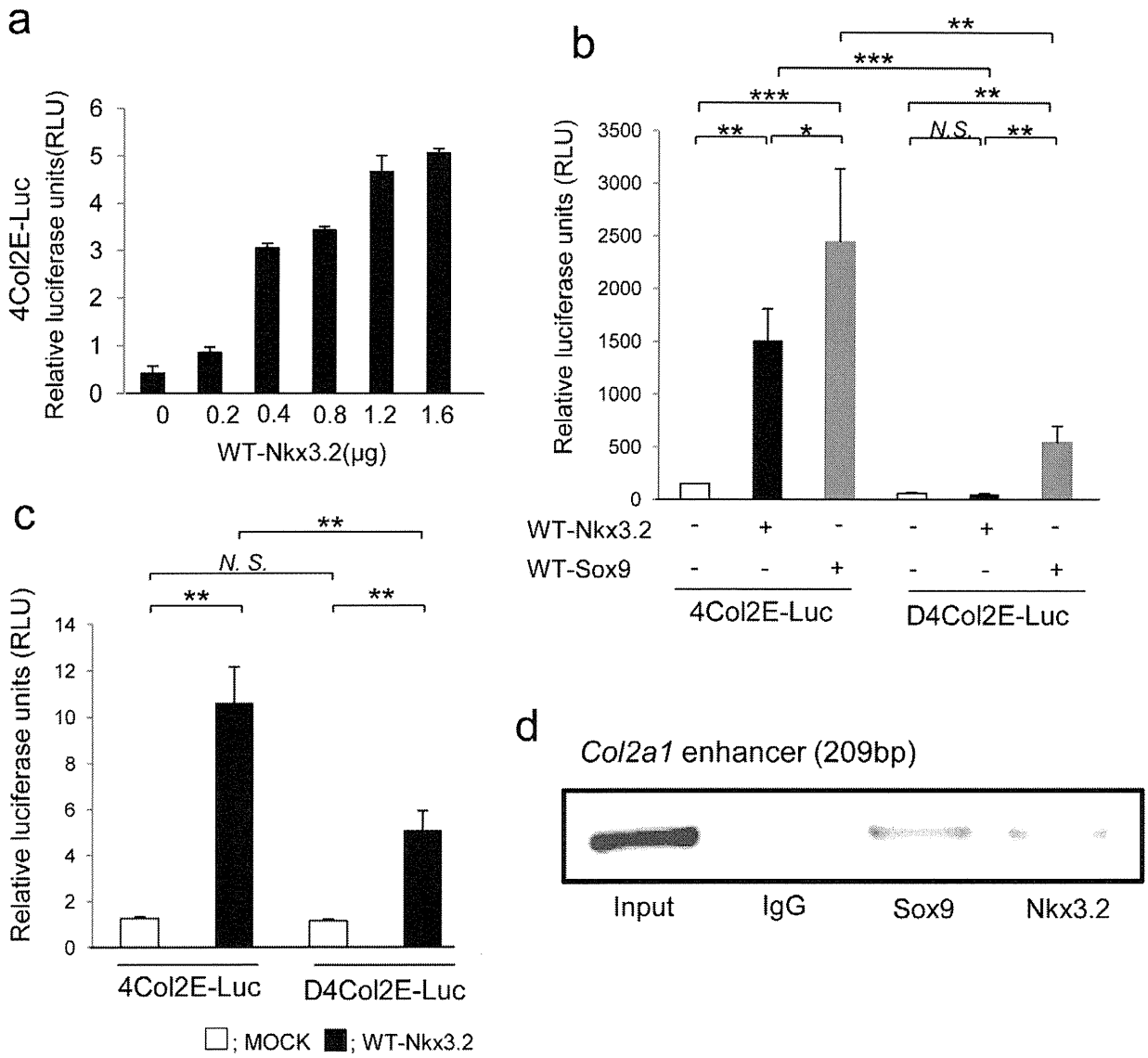

Figure 4. Nkx3.2 upregulated 48-bp *Col2a1* enhancer activity in C3H10T1/2 cells (**a** and **b**) and in N1511 cells (**c**) and binds to 48-bp *Col2a1* enhancer (**d**). **a** Transient transfection of Nkx3.2 showed does-dependent activation of 4Col2E-Luc. **b** Transcriptional activity of 4Col2E-Luc and D4Col2E-Luc using WT-Nkx3.2. Activation by WT-Sox9 is shown as a positive control. $*P<0.05$; $**P<0.01$; $***P<0.001$; *N.S.*, not significant. **c** Transient transfection of Nkx3.2 resulted in activation of the 4Col2E-Luc construct in N1511 cells. In contrast, the D4Col2E-Luc construct was not activated by Nkx3.2 overexpression. $**P<0.01$; *N.S.*, not significant. **d** Chromatin immunoprecipitation was performed using Nkx3.2, Sox9, and control antibodies in C3H10T1/2 cells. Products were obtained from PCR of immunoprecipitated chromatin with primers for the *Col2a1* enhancer. The sizes of the products are indicated. The first lane in each panel shows the PCR product obtained with chromatin input. Data are representative of three independent experiments.

doi:10.1371/journal.pone.0034703.g004

mobility shift assay and nuclear extracts of C3H10T1/2 cells transfected with WT-Nkx3.2 and 48-bp *Col2a1* probes and antibody targeting Nkx3.2. However, we could not detect a clear supershift; this result may have been due to some unsolvable difficulties (data not shown). Further confirmation is required to determine whether Nkx3.2 binds directly to the 48-bp *Col2a1* enhancer.

In conclusion, we have demonstrated for the first time that the Nkx3.2 transcription factor promoted primary chondrogenesis via binding to *Col2a1* enhancer element followed by upregulation of *Col2a1* transcription by both Sox9-dependent and Sox9-independent mechanisms.

Acknowledgments

The authors thank Dr. Riko Nishimura (Department of Biochemistry, Osaka University Graduate School, Faculty of Dentistry) for donating the wild-type Sox9 (WT-Sox9) plasmid. We also thank Osteopharma Inc. for supplying recombinant human BMP-2 and Dr. Hideto Watanabe and Dr. Nobuhiro Kamiya for donating the N1511 cells.

Author Contributions

Conceived and designed the experiments: YK MH KE KS JH AM. Performed the experiments: YK YH. Analyzed the data: YK YH KE. Contributed reagents/materials/analysis tools: YK. Wrote the paper: YK MH KE. Obtained permission for use of cell line: HY AM.

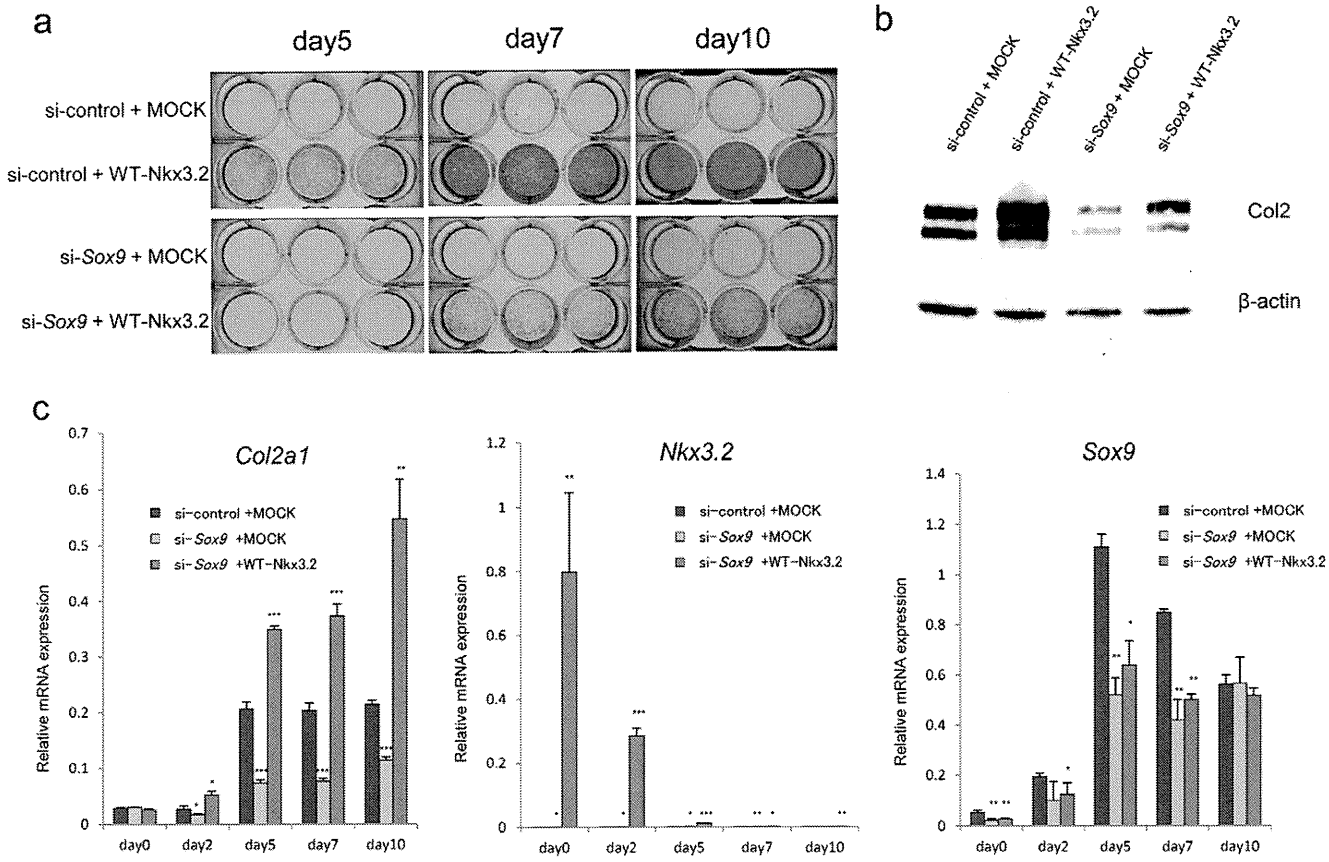

Figure 5. Overexpression of Nkx3.2 partially restored downregulation of GAG production (**a**), Col2 protein expression (**b**), *and Col2a1* mRNA expression (**c**) induced by si-*Sox9* in C3H10T1/2 cell culture. **a** After 24-h transfection with si-control (upper panels) or si-*Sox9* (lower panels), MOCK plasmid (upper wells) or WT-Nkx3.2 (lower wells) were transfected. After another 24-h culture (day 0), cells were stimulated with BMP-2 (300 ng/ml) for 5, 7, and 10 days. At each time point, cells were stained with alcian blue. **b** Western blot of Col2 on day 7. Overexpression of Nkx3.2 partially restored Col2 protein expression downregulated by si-*Sox9*. **c** Total RNA was extracted at each time point. Real-time PCR was used to assess *Col2a1*, *Nkx3.2*, *Sox9*, and *GAPDH* mRNA expression. Values are normalized to the level of *GAPDH* mRNA. Data are presented as means ± S.D. (n = 3). P values are evaluated v.s. si-control+MOCK group. $*P<0.05$; $**P<0.01$; $***P<0.001$; no marks represents no significant differences.
doi:10.1371/journal.pone.0034703.g005

References

1. Provot S, Schipani E (2005) Molecular mechanisms of endochondral bone development. Biochem Biophys Res Commun 328: 658–665.
2. Han Y, Lefebvre V (2008) L-Sox5 and Sox6 drive expression of the aggrecan gene in cartilage by securing binding of Sox9 to a far-upstream enhancer. Mol Cell Biol 28: 4999–5013.
3. Akiyama H (2008) Control of chondrogenesis by the transcription factor Sox9. Mod Rheumatol 18: 213–219.
4. Inada M, Yasui T, Nomura S, Miyake S, Deguchi K, et al. (1999) Maturational disturbance of chondrocytes in Cbfa1-deficient mice. Dev Dyn 214: 279–290.
5. Kim IS, Otto F, Zabel B, Mundlos S (1999) Regulation of chondrocyte differentiation by Cbfa1. Mech Dev 80: 159–170.
6. Hirao M, Tamai N, Tsumaki N, Yoshikawa H, Myoui A (2006) Oxygen tension regulates chondrocyte differentiation and function during endochondral ossification. J Biol Chem 281: 31079–31092.
7. Zeng L, Kempf H, Murtaugh LC, Sato ME, Lassar AB (2002) Shh establishes an Nkx3.2/Sox9 autoregulatory loop that is maintained by BMP signals to induce somitic chondrogenesis. Genes Dev 16: 1990–2005.
8. Lengner CJ, Hassan MQ, Serra RW, Lepper C, van Wijnen AJ, et al. (2005) Nkx3.2-mediated repression of Runx2 promotes chondrogenic differentiation. J Biol Chem 280: 15872–15879.
9. Tribioli C, Lufkin T (1999) The murine Bapx1 homeobox gene plays a critical role in embryonic development of the axial skeleton and spleen. Development 126: 5699–5711.
10. Lettice LA, Purdie LA, Carlson GJ, Kilanowski F, Dorin J, et al. (1999) The mouse bagpipe gene controls development of axial skeleton, skull, and spleen. Proc Natl Acad Sci U S A 96: 9695–9700.
11. Hellemans J, Simon M, Dheedene A, Alanay Y, Mihci E, et al. (2009) Homozygous inactivating mutations in the NKX3-2 gene result in spondylo-megaepiphyseal-metaphyseal dysplasia. Am J Hum Genet 85: 916–922.
12. Akazawa H, Komuro I, Sugitani Y, Yazaki Y, Nagai R, et al. (2000) Targeted disruption of the homeobox transcription factor Bapx1 results in lethal skeletal dysplasia with asplenia and gastroduodenal malformation. Genes Cells 5: 499–513.
13. Aszodi A, Chan D, Hunziker E, Bateman JF, Fassler R (1998) Collagen II is essential for the removal of the notochord and the formation of intervertebral discs. J Cell Biol 143: 1399–1412.
14. Kamiya N, Jikko A, Kimata K, Damsky C, Shimizu K, et al. (2002) Establishment of a novel chondrocytic cell line N1511 derived from p53-null mice. J Bone Miner Res 17: 1832–1842.
15. Lefebvre V, Zhou G, Mukhopadhyay K, Smith CN, Zhang Z, et al. (1996) An 18-base-pair sequence in the mouse proalpha1(II) collagen gene is sufficient for expression in cartilage and binds nuclear proteins that are selectively expressed in chondrocytes. Mol Cell Biol 16: 4512–4523.
16. Yamashita S, Andoh M, Ueno-Kudoh H, Sato T, Miyaki S, et al. (2009) Sox9 directly promotes Bapx1 gene expression to repress Runx2 in chondrocytes. Exp Cell Res 315: 2231–2240.
17. Kim DW, Kempf H, Chen RE, Lassar AB (2003) Characterization of Nkx3.2 DNA binding specificity and its requirement for somitic chondrogenesis. The Journal of biological chemistry 278: 27532–27539.
18. Lefebvre V, Li P, de Crombrugghe B (1998) A new long form of Sox5 (L-Sox5), Sox6 and Sox9 are coexpressed in chondrogenesis and cooperatively activate the type II collagen gene. The EMBO journal 17: 5718–5733.

19. Bernard P, Tang P, Liu S, Dewing P, Harley VR, et al. (2003) Dimerization of SOX9 is required for chondrogenesis, but not for sex determination. Human molecular genetics 12: 1755–1765.
20. Tsuda M, Takahashi S, Takahashi Y, Asahara H (2003) Transcriptional co-activators CREB-binding protein and p300 regulate chondrocyte-specific gene expression via association with Sox9. The Journal of biological chemistry 278: 27224–27229.
21. Kawakami Y, Tsuda M, Takahashi S, Taniguchi N, Esteban CR, et al. (2005) Transcriptional coactivator PGC-1alpha regulates chondrogenesis via association with Sox9. Proceedings of the National Academy of Sciences of the United States of America 102: 2414–2419.
22. Furumatsu T, Tsuda M, Yoshida K, Taniguchi N, Ito T, et al. (2005) Sox9 and p300 cooperatively regulate chromatin-mediated transcription. The Journal of biological chemistry 280: 35203–35208.
23. Furumatsu T, Tsuda M, Taniguchi N, Tajima Y, Asahara H (2005) Smad3 induces chondrogenesis through the activation of SOX9 via CREB-binding protein/p300 recruitment. The Journal of biological chemistry 280: 8343–8350.
24. Park M, Yong Y, Choi SW, Kim JH, Lee JE, et al. (2007) Constitutive RelA activation mediated by Nkx3.2 controls chondrocyte viability. Nature cell biology 9: 287–298.

Efficient modification of the surface properties of interconnected porous hydroxyapatite by low-pressure low-frequency plasma treatment to promote its biological performance

2012 J. Phys. D: Appl. Phys. 45 372001

(http://iopscience.iop.org/0022-3727/45/37/372001)

IOP PUBLISHING
IOP FTC
JOURNAL OF PHYSICS D: APPLIED PHYSICS
J. Phys. D: Appl. Phys. **45** (2012) 372001 (5pp)
doi:10.1088/0022-3727/45/37/372001

FAST TRACK COMMUNICATION

Efficient modification of the surface properties of interconnected porous hydroxyapatite by low-pressure low-frequency plasma treatment to promote its biological performance

Dae-Sung Lee[1], Yu Moriguchi[2], Akira Myoui[2], Hideki Yoshikawa[2] and Satoshi Hamaguchi[1]

[1] Center for Atomic and Molecular Technologies, Graduate School of Engineering, Osaka University, 2-1 Yamadaoka, Suita, Osaka 565-0871, Japan
[2] Department of Orthopaedics, Graduate School of Medicine, Osaka University, 2-2 Yamadaoka, Suita, Osaka 565-0871, Japan

E-mail: dslee@ppl.eng.osaka-u.ac.jp

Received 5 June 2012, in final form 12 August 2012
Published 29 August 2012
Online at stacks.iop.org/JPhysD/45/372001

Abstract
Dielectric barrier discharge plasma treatment at low pressure is found to significantly improve the biological performance of artificial bones made of interconnected porous calcium hydroxyapatite (IP-CHA). One of the essential parameters associated with their biological performance is hydrophilicity of their exterior surfaces as well as surfaces of inner pores. It is found that plasma treatment at low pressures is highly effective in making the inner pore surfaces more hydrophilic. Preliminary *in vivo* experiments of plasma-treated IP-CHA artificial bones in rats have shown fast formation of blood vessels in their inner pores, implying the increase in osteoconductivity due to the plasma treatment.

(Some figures may appear in colour only in the online journal)

Over the past years, considerable attention has been directed towards plasma biology and medicine, which are rapidly growing new areas of non-thermal plasma science and engineering. In medical applications, plasmas may be used for direct treatment of living tissues, which includes, for instance, sterilization, blood coagulation, wound healing and cure of skin deceases, or for indirect treatment, in which plasma-treated materials are brought into contact with living tissues for medical treatment. In direct treatment, plasmas need to be generated in the environment where the tissues to be treated exist and therefore their operation pressure needs to be atmospheric pressure [1–3]. In indirect treatment, on the other hand, low-pressure plasmas can be used and may be more effective in processing the materials, depending on the requirements and conditions for medical use.

In this paper, we shall present our recent study on plasma modification of artificial bone surfaces, which may be categorized as an indirect treatment mentioned above. Currently, a variety of biomaterials are available for bone grafting. Some of such biomaterials have structures and chemical compositions similar to those of natural bones and are effective in bone tissue regeneration [4, 5]. For example, calcium phosphate based materials such as β-TCP (tricalcium phosphate) and IP-CHA (interconnected porous calcium hydroxyapatite), which have similar chemical composition to natural bones and also function as scaffolds for bone

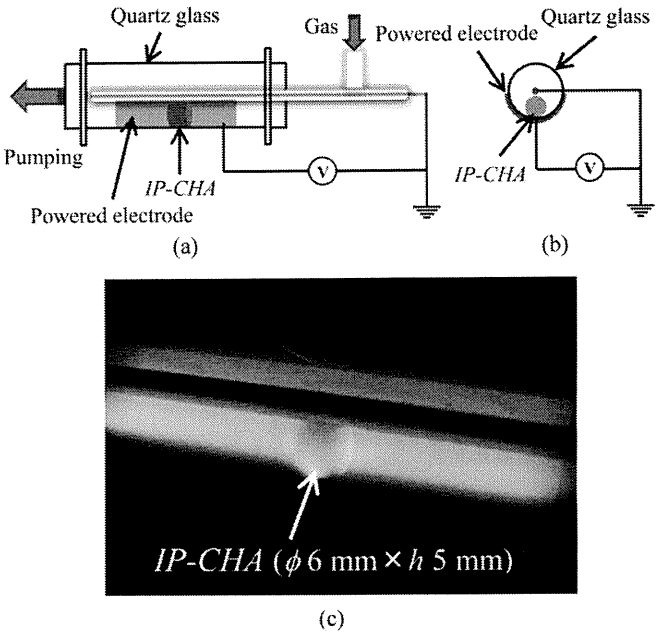

Figure 1. Schematics of the discharge system used in this study. (*a*) A side (plan) view of the discharge chamber and (*b*) its cross section, neither of which is drawn to scale. (*c*) A photograph of a typical discharge with a He/O_2 gas admixture with a pressure ratio of 5 : 1, total pressure of 0.6 kPa, an operating voltage (zero-to-peak) of 2.1 kV and a frequency of 40 kHz. An IP-CHA disc of 6 mm diameter (ϕ) and 5 mm height (h) is seen in the discharge chamber in (*c*).

tissue regeneration, are known to have high osteoconductivity, osteoinductivity and high ability to facilitate osteogenesis [5]. Artificial bones made of such materials are now widely used for bone grafting clinically but have not yet replaced autologous bone grafts completely. There is still room for significant improvement of artificial bones [6] that are currently available in the market.

For example, artificial bones made of IP-CHA are known to have mechanical strength superior to β-TCP and therefore can serve better as scaffolds for osteogenic cells [7–10]. However, their biocompatibility is yet to match that of autografts and can be improved if the hydrophilicity of IP-CHA surfaces, especially that of the inner pore surfaces, can be increased [11]. In this study, we examine plasma surface treatment as a means to improve hydrophilicity of IP-CHA artificial bones. In particular, we focus on the use of low-pressure plasmas for IP-CHA surface treatment.

We now discuss our experimental setup and methodology. The samples processed in this study are IP-CHA discs with 72% porosity in volume, an average pore diameter of 150 μm, and an average interpore-connection diameter of 40 μm. The dimensions of each disc are 6 mm in diameter and 5 mm in height. Such IP-CHA discs are suitable for small animal experiments [11]. More details of IP-CHA used may be found in [7].

Schematic diagrams of the plasma system used in this work are shown in figure 1, where a side view of the discharge chamber, its cross section, and a photograph of a typical discharge are given in (*a*), (*b*) and (*c*), respectively. In (*a*) and (*b*), the figures are not drawn to scale. The discharge system consists of a 12 cm long circular quartz glass tube with inner and outer diameters of 1.7 cm and 2.1 cm, respectively, a powered electrode made of a Cu film placed around the tube and a metal (SUS) rod inserted at the centre of the quartz tube that functions as the grounded electrode. The Cu electrode attached to the outside of the quartz tube was powered by a 40 kHz sinusoidal voltage with an amplitude of 2.1 kV. The individual gases can be independently controlled and adjusted to maintain a desired gas pressure while the system is pumped by a rotary pump. A photograph of figure 1(*c*) shows an overall uniform and stable glow discharge formed in this system with a He/O_2 admixture gas (with the pressure ratio of 5 : 1) at the total pressure 0.6 kPa.

To evaluate the hydrophilicity of internal pores of IP-CHA, we have observed penetration of water (which contains a contrast medium (CM)) into an IP-CHA disc via x-ray computerized tomography (CT). In experiments reported in this paper, before the observation of hydrophilicity, each IP-CHA disc was entirely immersed in deionized (DI) water containing a CM (6% Oypalomin in DI water) for 10 min and then placed in a micro-CT system (SMX-100CT-SV, Shimadzu). The disc was scanned at 70 μm intervals by x-rays emitted from a radiation source. The x-rays are shielded by a brass film placed in front of the radiation source, which eliminates interface scattering and beam hardening effects. Three-dimensional (3D) image data showing the locations of the CM in an IP-CHA disc were reconstructed from 2D micro-CT data with the use of the TRI3DBON software package (Ratoc System Engineering).

In a typical experiment, a sample, i.e. an IP-CHA disc, was placed in a plasma generated in the system discussed above for a given duration at a specified pressure. Then the sample was taken out from the system and the level of water penetration into the sample was observed with the micro-CT system. Figure 2 presents the micro-CT 2D images of the IP-CHA discs treated under various conditions. The image of an IP-CHA disc shown in figure 2 is a 2D CT image of the disc cross section at the mid-plane. It is a combined image of three separate images, each of which represents the location of hydroxyapatite (HA), voids (i.e. empty space representing unfilled pores in the IP-CHA disc) or CM contained in water (i.e. water filled pores). Figure 2(*a*) shows an example, where HA, voids and CM are separately depicted in yellow, blue and pink, respectively, and their combined image is given on the right. If no penetration of CM solution occurs, the image of CM will be missing in the combined image. By observing the distribution of CM at different heights (i.e. thicknesses) of the disc, we have evaluated the volume of CM penetration, which reflects the hydrophilicity of the inner pore surfaces.

Figure 2(*b*) shows the 2D cross sectional images of the IP-CHA discs treated by the plasma with different plasma exposure durations (i.e. treatment times). Similarly figure 2(*c*) shows the images with different operating gas pressures. The other conditions are the same as those mentioned above or as indicated in the figure. The gas is an admixture of He/O_2 with a pressure ratio of 5 : 1. A dashed circle in each figure represents the region in which no CM is observed. It is seen that the depth of water penetration into the disc increases generally with the

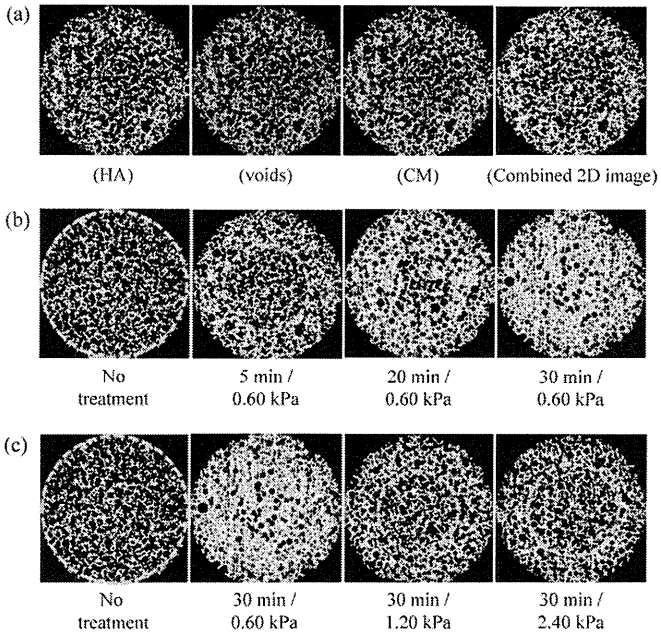

Figure 2. Micro-CT 2D images of the IP-CHA discs ($\phi 6 \times h5\,\mathrm{mm}^2$) with or without plasma treatment. Each image represents the cross section at the mid-plane of height (i.e. thickness) of the cylindrical disc. Before each measurement, the disc is entirely immersed in CM solution (6% Oypalomin with DI water) for approximately 10 min. Each image is composed of three parts as shown in (*a*); yellow for hydroxyapatite (i.e. HA), blue for empty space (i.e. unfilled pores) and pink for the CM solution (i.e. CM filled pores). The plasma conditions for (*a*) are 5 min plasma treatment at 0.6 kPa. In (*b*) and (*c*), the operating conditions for images of IP-CHA discs treated under different plasma conditions are denoted below the images. A dashed circle in each figure represents the region in which no CM solution is observed.

treatment time. Also, the images indicate that the penetration depth within a fixed treatment time increases as the pressure decreases unless the pressure is very low. Figure 3 shows the 3D images derived from the set of 2D cross-sectional images at different heights of an untreated disc and a disc treated for 30 min at a pressure of 0.6 kPa. It is seen that, with plasma treatments, most pores become filled with the CM solution, which indicates the increase in hydrophilicity of the inner pore surfaces.

We define the penetration fraction p of the CM solution as

$$p = \frac{V_{\mathrm{CM}}}{V_{\mathrm{V}}} \times 100,$$

where V_{CM} and V_{V} represent the volume of the CM solution and the volume of voids (i.e. pores) inside the IP-CHA disc. The value of V_{CM} was obtained by counting the number of pixels representing the CM in the 3D micro-CT image. The value of V_{V} is the total volume of voids, i.e. 72% porosity of the nominal volume occupied by the IP-CHA disc determined by its diameter and height. If all surfaces of the IP-CHA disc are highly hydrophilic, we expect the penetration fraction p becomes close to 100% after the disc is immersed in the solution for a sufficiently long period. During the immersion, however, trapped air in pores may impede or even prevent further penetration of the solution into pores unless

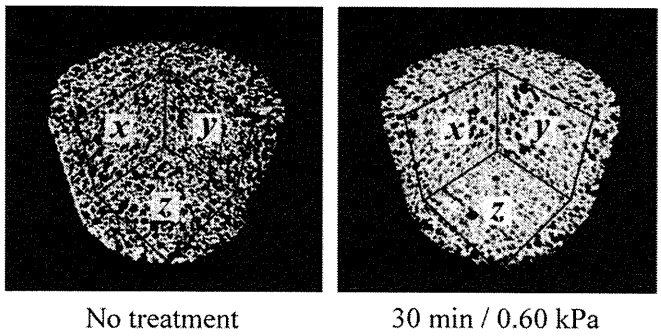

Figure 3. Sample 3D images of the untreated (left) and plasma-treated (right) IP-CHA discs. The treatment time and the total pressure of the plasma are indicated below the right figure.

it is ventilated by some means or absorbed by the solution. Therefore, the penetration fraction p shown here may not completely reflect the hydrophilicity of the inner pore surfaces.

Figure 4 shows the penetration fraction p as functions of (*a*) treatment time and (*b*) total pressure. The dashed lines are drawn as a guide to the eye. It is seen in figure 4(*a*) that the penetration fraction p increases with the treatment time but saturates at around 20–30 min under the conditions examined here. From the data shown here it is not clear whether this saturation is due to the lack of sufficient hydrophilicity in the innermost pores or the prevention of solution penetration by trapped air during the immersion process for measurement. However, a close examination has indicated that hydrophilicity in the inner pore did not improve under the conditions discussed here and the penetration fraction p presented here correctly indicates the level of hydrophilicity in the inner pores.

The pressure dependence of the penetration fraction p given in figure 4(*b*) shows that the inner pores are more easily processed at a lower pressure unless the pressure becomes so low that the processing gas would be deficient for surface modification. This result may indicate better permeation of gaseous reactive species in pores at a lower pressure. However, it may also reflect the fact that, at higher pressures (especially at 1 kPa or above), the plasma becomes more localized near the metal ground electrode and therefore the production rate and spatial distributions of charged species and reactive species also change. Based on the experimental observations, we have found that, under the conditions examined here, the optimal conditions for treatment time and pressure are about 30 min and 0.6 kPa, respectively.

An increase in the hydrophilicity of IP-CHA by plasma treatment can be easily seen if one places the IP-CHA disc on water surface. An untreated IP-CHA disc of the size discussed here floats on water and we have confirmed that it remains floating for more than 10 months at this moment. On the other hand, a disc treated under the optimal conditions discussed above immediately sinks. We have also confirmed using a contact-angle measurement system (PGX, FIBRO system ab) that the hydrophilicity on the surface of (non-porous) HA increases by the plasma treatment. For example, under ambient conditions at a temperature of 25 ± 1 °C and a relative humidity of 50 ± 5%, the contact angle of a DI water droplet on a (non-porous) HA sample without plasma treatment was about 85°

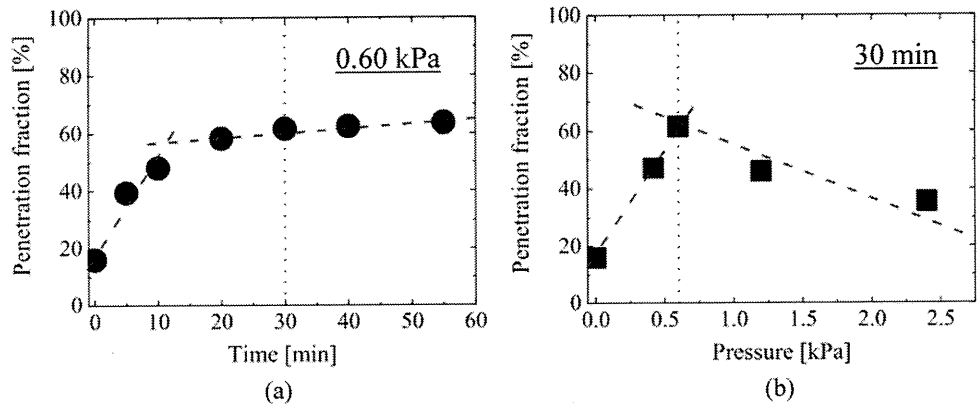

Figure 4. Penetration fraction p as functions of (a) plasma treatment time and (b) gas pressure. The fixed parameters are indicated in the figures. The red dashed lines are drawn as a guide to the eye.

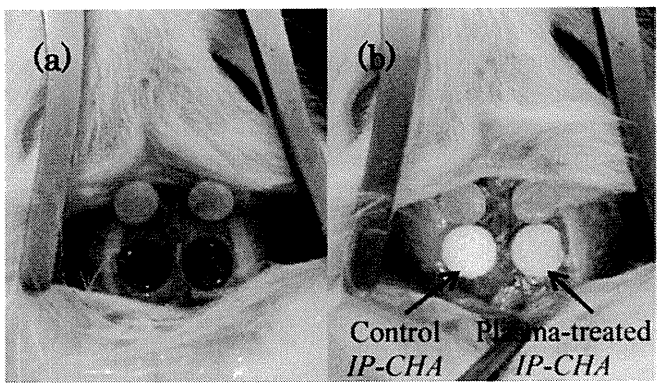

Figure 5. A Photograph of two calvarial bone defects of a rat (a) and a photograph taken right after plasma-treated (right) and untreated (left) IP-CHA discs were inserted into the bone defects for bone grafting (b). In (b), rapid absorption of blood is seen in the plasma-treated IP-CHA.

whereas that of a (non-porous) HA sample treated by an oxygen plasma for an extended period was nearly 0°. Such a high hydrophilicity is often considered as a favourable factor for biocompatibility of blood-contacting implant materials [12].

We have also performed preliminary *in vivo* study of bone grafting of rat calvaria using the plasma-treated IP-CHA discs. Figure 5 shows a photograph of two calvarial bone defects of a rat (a) and a photograph taken right after plasma-treated (right) and untreated (left) IP-CHA discs were inserted into the bone defects for bone grafting (b). In (b), rapid absorption of blood is seen in the plasma-treated IP-CHA. After a few weeks of bone grafting, the experiments have shown fast formation of blood vessels in the inner pores of the plasma-treated IP-CHA, implying the increase in osteoconductivity due to the plasma treatment. Details of this *in vivo* study will be presented elsewhere.

So far we have reported the results of IP-CHA plasma treatment with a fixed pressure ratio of He and O_2 gases. However, our experiments with different O_2 partial pressures as well as our preliminary analyses of IP-CHA surfaces by x-ray photoelectron spectroscopy (XPS) (the results of which are not shown here) suggest the importance of oxygen in the plasma for the surface treatment. In addition, we conjecture that the presence of water (moist) in the plasma also plays an important role as a source for the supply of hydrogen or hydroxyl groups that modify the surface. We have not yet fully understood the surface reactions responsible for the increase in hydrophilicity on IP-CHA surfaces by the plasma treatment and its examination is deferred to a future study.

We have also shown that surface modification (i.e. hydrophilization) occurs inside the interconnected inner pores. The modification of inner pore surfaces is shown to become less effective as the gas pressure for the plasma increases. At lower pressures, the collision mean paths of reactive species increase and therefore typically the transport distances of reactive species are expected to become longer. However, it is not clear whether this applies to the transport in capillary tubes (i.e. interconnected pores in our case) as the collision of reactive species with a material wall can be more frequent than collisions between gaseous particles at low pressures. In the case examined here, the nature of discharge also changes when the pressure is around 1 kPa or higher. If the pressure is sufficiently lower than 1 kPa, the sample IP-CHA disc is fully immersed in the plasma, whereas if the pressure is at 1 kPa or higher, the plasma is more localized around the grounded electrode. Transport of reactive species in capillary tubes in low-pressure plasmas needs to be examined further in order for us to understand the optimal conditions for plasma treatment of inner pore surfaces.

In conclusion, surface modification of IP-CHA artificial bone discs by plasmas of a He/O_2 gas admixture at a pressure of around 0.6 kPa has successfully increased their hydrophilicity, including that of the inner pore surfaces. The higher penetration fraction p of IP-CHA achieved by the plasma treatment is likely to lead to better biocompatibility of the artificial bones made of IP-CHA and possibly to better osteoconductivity. Our preliminary *in vivo* experiments using the IP-CHA discs as artificial bone grafts to rat calvaria have indicated that plasma treatment of IP-CHA studied in this work is likely to improve their biocompatibility and osteoconductivity.

Acknowledgment

The authors thank Denshi Giken Co. Ltd for their support with contact-angle measurements.

References

[1] Fridman A 2008 *Plasma Chemistry* (Cambridge: Cambridge University Press)
[2] Laroussi M 2002 *IEEE Trans. Plasma Sci.* **30** 1409
[3] Ehlbeck J, Schnabel U, Polak M, Winter J, Woedtke T, Brandenburg R, Hagen T and Weltmann K-D 2011 *J. Phys. D: Appl. Phys.* **44** 013002
[4] Hench L-L 1998 *J. Am. Ceram. Soc.* **81** 1705
[5] Ahmed W, Ali N and Öchsner A (ed) 2008 *Biomaterials and Biomedical Engineering* (Dumten-Zurich: Trans Tech Publications)
[6] Lee D-S, Moriguchi Y, Okada K, Myoui A, Yoshikawa H and Hamaguchi S 2011 *IEEE Trans. Plasma Sci.* **39** 2166
[7] Tamai N, Myoui A, Kudawara I, Ueda T and Yoshikawa H 2010 *J. Orthop. Sci.* **15** 560
[8] Deie M, Ochi M, Adachi N, Nishimori M and Yokota K 2008 *Knee Surg. Sports Traumatol. Arthrosc.* **16** 753
[9] Ito Y, Tanaka N, Fujimoto Y, Yasunaga Y, Ishida O, Agung M and Ochi M 2004 *J. Biomed. Mater. Res.* A **69** 454
[10] Tamai N, Myoui A, Tomita T, Nakase T, Tanaka J, Ochi T and Yoshikawa H 2002 *J. Biomed. Mater. Res.* **59** 110
[11] Yamasaki N, Hirao M, Nanno K, Sugiyasu K, Tamai N, Hashimoto N, Yoshikawa H and Myoui A 2009 *J. Biomed. Mater. Res. B Appl. Biomater.* **91** 788
[12] Yoshikawa H and Myoui A 2005 *J. Artif. Organs* **8** 131